Desalination 257 (2010) 163–169

Contents lists available at ScienceDirect

Desalination

journal homepage: www.elsevier.com/locate/desal

Performance of magnesium oxide-coated bentonite in removal process of copper ions from aqueous solution

E. Eren [a,*], A. Tabak [b], B. Eren [a]

[a] Bilecik University, Faculty of Arts and Science, Department of Chemistry, Bilecik, Turkey
[b] Rize University, Faculty of Arts and Science, Department of Chemistry, Rize, Turkey

ARTICLE INFO

Article history:
Received 6 November 2009
Received in revised form 12 February 2010
Accepted 16 February 2010
Available online 19 March 2010

Keywords:
Bentonite
Adsorption
Thermodynamic
Clay
Cu(II)

ABSTRACT

This paper presents the adsorption of Cu(II) ions from aqueous solution on modified Unye bentonite. Adsorption of Cu(II) ions by magnesium oxide-coated bentonite (MCB) sample was investigated as a function of the initial Cu (II) concentration, solution pH, ionic strength, temperature and inorganic ligands (Cl^-, SO_4^{2-}, and HPO_4^{2-}). Changes in the surfaces and structure were characterized by means of XRD and N_2 gas adsorption data. The Langmuir monolayer adsorption capacity of MCB in 0.1 M KNO_3 solution was estimated as 58.44 mg/g. ΔG, ΔH and ΔS values were evaluated for MCB to be −9.50 kJ/mol (at 303 K), 43.81 kJ/mol and 175.85 J/mol K.

1. Introduction

The contamination of water by heavy metals through the discharge of industrial wastewater is a worldwide environmental problem. Removal of heavy metal ions from wastewater in an effective manner has become an important issue today. The main heavy metal removal methods are chemical precipitation, membrane filtration, ion exchange and adsorption [1]. Adsorption process provides an attractive alternative treatment to other removal techniques because it is more economical and readily available. A lot of non-conventional, low-cost and easily obtainable adsorbents have been tested for heavy metal removal such as clay minerals [2–5], biomaterials [6–9] and industrial solid wastes [10–13]. Those studies indicated that the adsorption capacity of most low-cost materials is much less effective than that of commercial adsorbents.

Bentonite is a natural clay that is found in many places of the world. Any clay of volcanic origin that contains montmorillonite is referred to as bentonite. It belongs to the 2:1 clay family, the basic structural unit of which is composed of two tetrahedrally coordinated sheets of silicon ions surrounding a sandwiched octahedrally coordinated sheet of aluminum ions. The isomorphous substitution of Al^{3+} for Si^{4+} in the tetrahedral layer and Mg^{2+} or Fe^{3+} for Al^{3+} in the octahedral layer results in a net negative surface charge on the clay [14]. Also, montmorillonite have amphoteric pH-dependent charges at the edges, high exchange capacity and different modes of aggregation [14,15]. Amphoteric edge surfaces of the montmorillonite provide sites for the adsorption of cations. This character of montmorillonite makes it a potential adsorbent for the adsorption of heavy metal from aqueous solutions.

The heavy metal adsorption onto iron or manganese oxide modified adsorbents has received wider attention than that of magnesium oxide modified adsorbents [16–21]. But, using MgO in the adsorption proceseses have many advantages such as its cost is much lower than that of iron and manganese oxides, MgO has minimal environmental impact, and Mg^{2+} is non-polluting and can be easily obtained from aqueous medium. For these reasons, MgO can be used as a promising mineral for the adsorption of heavy metals due to its high capacity for heavy removal when exposed to an initial acidic solution. In the present work, a cheap, readily available and effective adsorbent material has identified bentonite as a potentially attractive adsorbent for the treatment of Cu(II) ions contaminated with aqueous solutions after modification with magnesium oxide. Since there is a huge deposit of bentonite, there is a great potential for its utilization in wastewater treatment. The main objective of this study was to investigate the feasibility of using magnesium oxide modified bentonite for the maximum removal of Cu(II) ions from aqueous solutions.

2. Experimental

2.1. Reagents

All reagents used were of analytical purity. Synthetic solutions were prepared from concentrated stock solutions (Merck). A stock solution of Cu(II) was prepared by dissolving required amount of $Cu(NO_3)_2$

* Corresponding author. Tel.: +90 228 2160101; fax: +90 228 2160287.
E-mail address: erdal.eren@bilecik.edu.tr (E. Eren).

0011-9164/$ – see front matter © 2010 Elsevier B.V. All rights reserved.
doi:10.1016/j.desal.2010.02.028

(Merck) in double distilled water. HNO_3 and NaOH were obtained from Merck and used for pH value adjustment. Other agents used, such as NaCl, $NaNO_3$, Na_2SO_4, Na_3PO_4, and $Mg(NO_3)_2$ were all of analytical grade and all solutions were prepared with double distilled water.

RB had a mineral composition of 76% montmorillonite, 8% quartz, 12% dolomite and 4% other minerals. Whiteness was found to be 85%. RB was composed of 62.70% SiO_2, 20.10% Al_2O_3, 2.16% Fe_2O_3, 2.29% CaO, 3.64% MgO, 0.27% Na_2O, 2.53% K_2O, 0.21% TiO_2, and 0.02% P_2O_5. The ignition loss of the RB at 1273 K was also found to be 6.1%. The cation exchange capacity (CEC), determined with triethanolamine-buffered $BaCl_2$ solution (c = 0.1 M) followed by a reexchange with aqueous $MgCl_2$ solution (c = 0.1 M), is 0.65 mmol/g [22]. The total pore volume value is 0.07 cm^3/g, the micropores contribute to 11.42% of the total pore volume. The average pore diameter is 8.11 nm.

2.2. Preparation and characterization of RB and MCB

Preparation of RB: The RB sample (from Unye, Turkey) was ground and washed in deionized water several times at a 1:10 bentonite/water ratio. The mixture was stirred for 3 h and then kept standing overnight, followed by separation, washing and drying at 60 °C.

Preparation of MCB: Magnesium nitrate and sodium hydroxide were mainly used in the modification of RB to enhance the adsorption capacity of RB. 20 g of RB were immersed in sufficient 2.0 M sodium hydroxide and temperature of the reaction mixture was maintained at 90 °C for 4 h. The base activated RB was dispersed into 150 mL of 0.1 M $Mg(NO_3)_2$ aqueous solution. 300 mL of 0.1 M NaOH aqueous solution was added slowly with a drop rate of 1 mL/hour. The titration was carried out under nitrogen flow throughout the procedure to minimize unexpected reactions e.g. formation of carbonate salts. The obtained powder was rinsed with 0.01 M HCl aqueous solution to remove the excess $Mg(OH)_2$ precipitated on the outher surface of the clay and further washed with deionized water. Then, this sample was heated for 4 h in air at 700 K. The thermal treatment of mixed solids in air at 700 K leads to the formation of MgO [23].

The mineralogical compositions of the RB and MCB samples were determined from the X-ray diffraction (XRD) patterns of the products taken on a Rigaku 2000 automated diffractometer using Ni filtered CuK_α radiation. XRD analysis of the bentonite was performed using the three-principal lines [24]. The surface areas were calculated by the BET (Brunauer–Emmett–Teller) method. The BET surface area (S_{BET}), external surface area (including only mesopores $S_{ext.}$), micropores surface area ($S_{mic.}$), total pore volume (V_t) and average pore diameter (D_p) results obtained by applying the BET equation to N_2 adsorption at 77 K and Barret–Joymer–Halenda (BJH) equation to N_2 adsorption at 77 K are listed in Table 1.

2.3. Adsorption dependence on Cu(II) concentration

The adsorption of Cu(II) ions by bentonite samples was performed by a batch equilibrium technique at room temperature. Briefly, 0.050 g of bentonite sample and 20 mL of $Cu(NO_3)_2$ solution were added in 50 mL polyethylene test tubes. Ionic strength was controlled at 0.1 M KNO_3 and the pH of the system was maintained at 6.0. The initial Cu(II) concentrations varied from 0.01 to 1.0 mM. A 24-h contacting period was found to be sufficient to achieve equilibrium. The samples were allowed to equilibrate for 24 h, centrifuged at 4500 *g* for 20 min and then decanted. All the measurements were made in duplicate and the average values were reported. An experiment without adsorbent was performed to test possible adsorption and/or precipitation of Cu(II) onto the test tube walls. Preliminary experiments showed that Cu(II) losses due to the adsorption onto the test tubes were negligible. Adsorbed Cu (II) ions was calculated from the difference between the Cu(II) ions initially added to the system and that remaining in the solution after equilibration by a Unicam 929 model flame atomic absorption spectrophotometer, Cu(II): lamp current at 5 mA, wavelength at 324.8 nm, slit width at 0.5 nm, and optimum working range of 2–10.0 μg/mL; flame type air/acetylene, and fuel flow rate of 1.2 L/s. The dilutions induced by the pH controls were considered while computing the amount of Cu(II) ions adsorbed.

Table 1
Porous structure parameters of the RB and MCB samples.

Sample	S_{BET} (m^2/g)	$S_{ext.}$[a] (m^2/g)	$S_{mic.}$ (m^2/g)	V_t (cm^3/g)	$V_{mic.}$ (cm^3/g)	$V_{meso.}$ (cm^3/g)	D_p[b] (nm)
RB	57	19	38	0.084	0.010	0.074	5.72
MCB	30	10	20	0.065	0.005	0.060	7.82

[a] $S_{ext} = S_{meso}$.
[b] 4 *V*/*A* by BET.

2.4. Effect of ionic strength, pH, inorganic ligand and temperature

Adsorption experiments were carried out in polyethylene test tubes at 23 ± 2 °C by using the batch technique. The reaction mixture consisted a total of 50 mL containing 2 g/L adsorbent and the desired concentration of Cu(II). The background electrolyte solutions were 0.01 M, 0.05 M, and 0.1 M KNO_3. Solution pH was adjusted with 0.1 M HNO_3 or 0.1 M NaOH, such that the equilibrium solutions had pH values ranging from 3.0 to 6.5. The procedure of ionic strength, pH, inorganic ligand and temperature experiments was basically identical to that of equilibrium tests. For thermodynamic studies, the temperature that was varied from 303 K to 338 K at a constant pH of 6.0. 2 g/L of MCB with 38 mg/L Cu (II) solutions was employed for these experiments.

3. Results and discussion

3.1. Data processing

The adsorption capacity of Cu(II) ions adsorbed per gram adsorbent (mg/g) was calculated using the equation

$$q_e = (C_0 - C_e)V / m \quad (1)$$

The adsorption percentage of Cu(II) ions was calculated by the difference of initial and final concentration using the equation expressed as follow:

$$R = [(C_0 - C_e) / C_0]x100 \quad (2)$$

where q_e is the equilibrium concentration of Cu(II) ions on the adsorbent (mg/g), C_0 the initial concentration of the Cu(II) ions solution (mg/L), C_e the equilibrium concentration of the Cu(II) ions solution (mg/L), *m* the mass of adsorbent (g), *V* the volume of Cu(II) ion solutions (L), and *R* the retention of Cu(II) ions in % of the added amount.

In this study, the equilibrium experimental data for adsorbed Cu(II) ions on bentonite sample were analyzed using the Langmuir, Freundlich and Dubinin–Radushkevich (D–R) isotherm models. These isotherms are as follows:

(a) Langmuir isotherm model [25]:

$$C_e / q_e = C_e / q_m + 1 / K_L q_m \quad (3)$$

where C_e is equilibrium concentration of Cu(II) ions (mg/L) and q_e is the amount of the Cu(II) ions adsorbed (mg) by per unit of bentonite (g). q_m and K_L are the Langmuir constants related to the adsorption capacity (mg/g) and the equilibrium constant (mg/L), respectively.

(b) Freundlich isotherm model [26]:

$$\log q_e = \log K_F + (1 / n) \log C_e \quad (4)$$

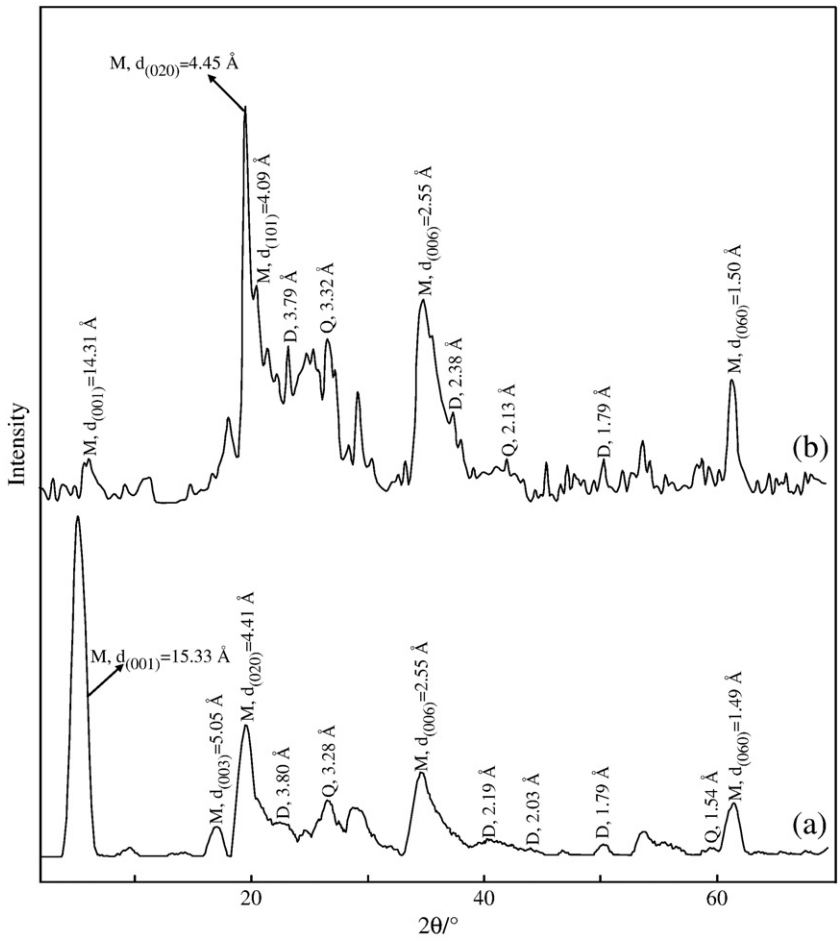

Fig. 1. The XRD patterns of the RB (a) and MCB (b) samples (M: montmorillonite, D: dolomite, Q: quartz).

where K_F and n are Freundlich constants related to adsorption capacity and adsorption intensity, respectively.

(c) D–R isotherm model [27]:

$$\ln q_e = \ln q_m - \beta\varepsilon^2 \quad (5)$$

where β is the activity coefficient related to mean adsorption energy (mol^2/J^2) and ε is the Polanyi potential ($\varepsilon = RT\ln(1+(1/C_e))$). The D–R isotherm is applied to the data obtained from the empirical studies. The mean adsorption energy, E (kJ/mol) is as follows:

$$E = 1/\sqrt{-2\beta} \quad (6)$$

This adsorption potential is independent of the temperature, but it varies depending on the nature of adsorbent and adsorbate.

Using the following equations, the thermodynamic parameters of the adsorption process can be determined from the experimental data:

$$lnK_d = \Delta S/R - \Delta H/RT \quad (7)$$

$$\Delta G = \Delta H - T\Delta S \quad (8)$$

$$K_d = q_e/C_e \quad (9)$$

where K_d is the distribution coefficient for the adsorption, ΔS, ΔH and ΔG are the changes of entropy, enthalpy and the Gibbs energy, q_e is the equilibrium concentration of Cu(II) ions on the adsorbent (mg/g), T (K) is the temperature, R ($J\,mol^{-1}\,K^{-1}$) is the gas constant, The values of ΔH and ΔS were determined from the slopes and intercepts of the plots of ln K_d vs. $1/T$.

3.2. Material characterization

The XRD patterns of the RS and MCB samples are presented in Fig. 1. Some of the structural properties of the MCB used in this study have been described in Eren at al. [28]. The authors demonstrated that the magnesium oxide-coating process has caused structural changes in the bentonite sample. The position of d_{001} peak of MCB sample shifted from 15.33 to 14.31 Å (Table 2). The intensities of the 001 and 006 reflections have been reduced, while the intensities of the 020 and 060 reflections have been increased significantly by the modification process. The new peaks situated at lower 2θ value (<6.17°) were likely to appear because of agglomeration of the MCB sheets [29]. MCB sample displays an increase of the background in the interval between 20 and 30°. The d_{003} reflection of *RB* at 5.05 Å ($2\theta = 17.52$) disappeared after the modification process.

Table 2
d-spacing and intensity values of reflections for bentonite samples.

Reflection	RB	MCB
	d, Å	*d*, Å
d_{001}	15.33	14.31
d_{003}	5.05	–
d_{020}	4.42	4.45
d_{101}	–	4.05
d_{006}	2.55	2.55
d_{060}	1.49	1.49

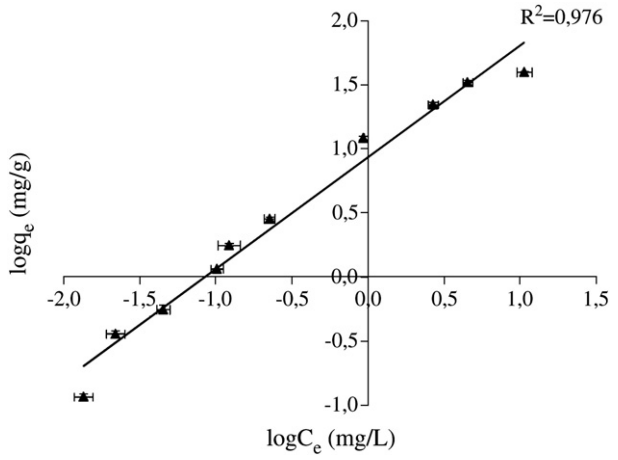

Fig. 2. Langmuir isotherm plot for the adsorption of Cu(II) ions onto the MCB sample. $T = 295.15$ K, initial pH = 6.0, $m = 2$ g/L. Error bars represent standard deviations from the average measurements.

Table 4
Adsorption results of Cu(II) ions from the literature by various adsorbents.

Adsorbent	pH	Temp. (*K*)	q_m (mg/g)	Ref. no
Çankırı bentonite	7.0	296	44.84	[1]
Organo-bentonite	5.5	323	56.55	[33]
Palygorskite	5–6	295	17.4	[31]
Acid-activ. palygorskite	6.0	303	32.24	[32]
Zeolite	–	303	8.97	[33]
Zeolite-cement mixture	–	298	23.25	[34]
Sawdust	–	308	4.94	[35]
Dye loaded sawdust	–	308	7.60	[35]
Diatomite	4.0	296	27.55	[36]
MnO-diatomite	4.0	296	55.56	[36]
Gran. act. carb. (GAC)	6.0	–	60	[37]
MnO-GAC	6.0	–	86	[37]
Bentonite	6.0	295	42.41	[38]
MnO-bentonite	6.0	295	105.38	[38]
Kaolinite	5.7	303	4.4	[39]
ZrO-kaolinite	5.7	303	3.0	[39]
TBA-kaolinite	5.7	303	3.2	[39]
Montmorillonite	5.7	303	28.8	[39]
ZrO-montmorillonite	5.7	303	7.1	[39]
TBA-montmorillonite	5.7	303	27.3	[39]
MCB	6.0	295	58.44	In this study

3.3. Adsorption isotherms and parameters

The equilibrium data for Cu(II) ions adsorption on bentonite samples were fitted to Langmuir equation (Eq. (3)). Linear plots of C_e/q_e vs. C_e (Fig. 2) were employed to determine the value of q_m (mg/g) and K_L (mg/L). The data obtained with the correlation coefficients (R^2) was listed in Table 3. The Langmuir monolayer adsorption capacity MCB was estimated as 58.44 mg/g, respectively (Table 3).

The adsorption capacities of the adsorbents for the removal of Cu (II) ions have been compared with those of other adsorbents reported in the literature and the values of adsorption capacities have been presented in Table 4. The values are reported in the form of monolayer adsorption capacity. The experimental data of the present investigation are comparable with the reported values [1,30–39]. Comparison of maximum experimental adsorption capacities of Cu(II) ions for metal oxide modified adsorbents were also given in Table 4 [36–39]. Maximum adsorption capacity of Cu(II) ions for metal oxide modified modified samples was approximately 1.5–2 times higher than that of the raw material [36–38]. From these observations, it appeared that the surface properties of RB could be improved upon modification of metal oxide as previously reported by other researchers [36–39].

Freundlich parameter (n) was related to the affinity between the adsorbate and the adsorbent and there is also an evidence of relation of this parameter with the solid-state properties of adsorbent. K_F relates the multilayer adsorption capacity and n intensity of adsorption, which varies with the heterogeneity of the adsorbent [40]. The constants in Table 3, K_F and n were calculated from Eq. (4) and Freundlich plots (Fig. 3). A high value of the intercept, K_F, is indicative of a high adsorption capacity [41]. A relatively $n \ll 1$ indicates that adsorption intensity is favorable over the entire range of concentrations studied, while $n > 1$ means that adsorption intensity is favorable at high concentrations but much less at lower concentrations [41,42]. In the adsorption system, n value is 1.16 which indicates that adsorption intensity is favorable over the entire range of concentrations studied.

A plot of $\ln q_e$ against ε^2 is given in Fig. 4. D–R isotherm constants, q_m for MCB was found to be 12.16 mg/g, respectively (Table 3). The difference of q_m derived from the Langmuir and D–R models is large. The difference may be attributed to the different definitions of q_m in the two models. In Langmuir model, q_m represents the maximum adsorption of metal ions at monolayer coverage, whereas it represents the maximum adsorption of metal ions at the total specific micropore volume of the adsorbent in D–R model. Thereby, the value of q_m derived from Langmuir model is higher than that derived from D–R model. The differences are also reported in previous studies [43–46]. In the mean adsorption energy, E is independent of the temperature, but it varies depending on the nature of adsorbent and adsorbate. The magnitude of E is used for estimating the type of adsorption mechanism. If the E value is between 8 and 16 kJ/mol, the adsorption process follows the chemical adsorption and if $E < 8$ kJ/mol, the adsorption process is of a physical nature [1,43–47]. The calculated values of E is 2.81 kJ/mol for MCB, and it is in the range of values for physical adsorption reactions. The similar results for the adsorption of Cr(III), Pb(II) and Zn(II) were reported by earlier workers [1,43].

3.4. Effects of ionic strength, pH and inorganic ligand

The adsorption of Cu(II) ions onto the MCB as a function of ionic strength and pH was shown in Fig. 5. The Cu(II) ion removals by MCB were observed over a range of initial pH values between 3 and 6.5. Increasing the ionic strength from 0.01 to 0.1 led to a significant decrease in the Cu(II) ion adsorptions. The percentage of Cu(II) ions adsorbed in the presence of 0.01 M KNO_3 at pH 6.5 is ≈91%, compared to 62% at the same pH but in the presence of 0.1 M KNO_3 for the MCB samples. This may be due to the following two reasons: i — the effect of ionic strength on metal adsorption may be explained by the formation of outer-sphere complexes since K^+ in the background electrolyte could compete with the metal ions adsorbed on the outer-sphere adsorption sites and could reduce the adsorption, whereas K^+ would not have competed for the inner-sphere sites [48]. ii — the electrostatic attraction seems to be a significant mechanism, as indicated by the results where

Table 3
Langmuir, Freundlich and D–R isotherm parameters for the adsorption of Cu(II) ions onto bentonite samples.

Sample	Langmuir isotherm constants			Freundlich isotherm constants			D–R isotherm constants		
	q_m (mg/g)	K_L (L/mg)	R^2	n	K_F ((mg/g)(L/mg)$^{1/n}$)	R^2	q_m (mg/g)	E (kJ/mol)	R^2
MCB	58.44 ± 0.46	0.22 ± 0.13	0.976	1.16 ± 1.13	8.93 ± 0.90	0.994	7.31 ± 0.80	2.81 ± 1.42	0.878

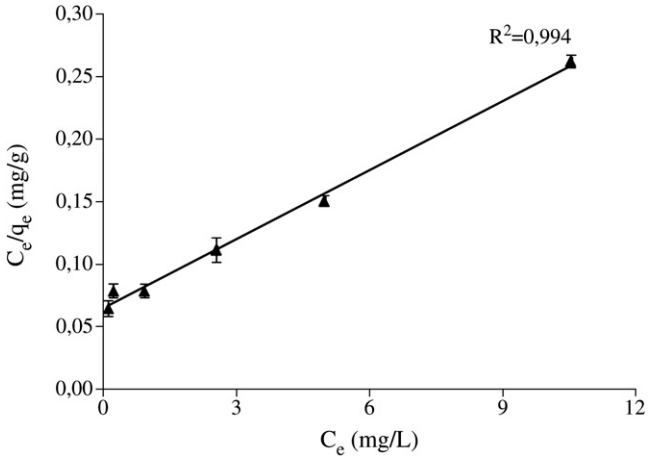

Fig. 3. Freundlich isotherm plot for adsorption of Cu(II) ions on the MCB sample. $T = 295.15$ K, initial pH = 6.0, m = 2 g/L. Error bars represent standard deviations from the average measurements.

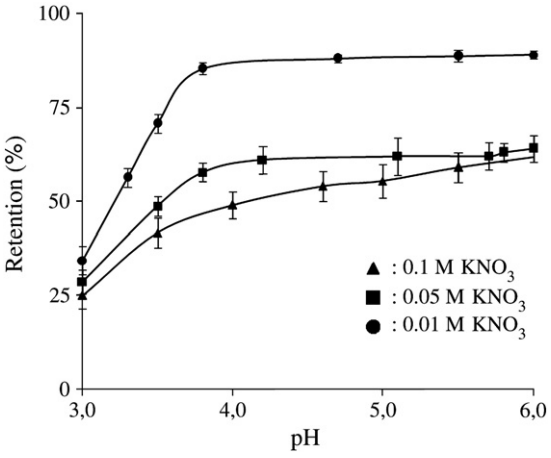

Fig. 5. Adsorption of Cu(II) ions (38 mg/L) by MCB (2 g/L) as function of pH and ionic strength. Error bars represent standard deviations from the average measurements.

at high ionic strength, the increased amount of KNO_3 can help to render the surface of the MCB not easily accessible to Cu(II) ions. According to the electrical diffuse double layer theory, when solid adsorbents are in contact with sorbate species in solution, they are bound to be surrounded by an electrical diffused double layer, the thickness of which is significantly expanded by the presence of electrolyte. Such expansion may be inhibited by the approaching MCB particles and Cu (II) cations.

The adsorption of Cu(II) ions by the MCB sample was influenced by the presence of Cl^-, SO_4^{2-} and HPO_4^{2-} (Fig. 6). It is clear that aqueous speciation influences Cu(II) ions adsorption in the inorganic ligand systems. The adsorbed Cu(II) ions in the presence of inorganic ligands may be also attributed to a high specifity of the surfaces for Cu(II) ions relative to ligands. The percentages of Cu(II) ions adsorbed in the 0.01 M SO_4^{2-} and HPO_4^{2-} systems at pH 6.5 are 58 and 54%, respectively, compared to 62% at the same pH but in the absence of these ligands. The decreased amount of adsorbed Cu(II) ions can be explained in terms of solution chemistry. These ions effectively decrease the degree of hydrolysis of Cu(II) ions by blocking some of the co-ordination positions. Also, the reduction in Cu(II) ion adsorptions on the MCB sample in the presence SO_4^{2-} and HPO_4^{2-} might be due to ion competition with the various Cu(II) species for adsorption sites {e.g. [XOH^+-SO_4^{2-} and XOH^+-HPO_4^{2-}]}. Fig. 6 also showed that the retention of Cu(II) ions by MCB surface was enhanced in the presence of 0.01 M Cl^- ligand. The percentage of Cu(II) ions adsorbed in the 0.01 *M* Cl^- system at pH 6.5 is 75% for the MCB sample. This result suggests that the observed Cu(II) ion adsorption behavior in the MCB suspensions is influenced by both aqueous speciation and surface ligand complexation of Cu(II) ions. The specifically adsorbed ligand enhances the Cu(II) ions' retention by the surface complexation of Cu(II) ions.

3.5. Thermodynamic studies

ΔG, ΔH and ΔS were reported for RB as −0.34 kJ/mol (at 303 K), 10.36 kJ/mol and 42 J/mol K, respectively [41]. In this work, these values were evaluated for MCB as −9.50 kJ/mol (at 303 K), 43.81 kJ/mol and 175.85 J/mol K, respectively (Table 5). The negative values for the Gibbs free energy change, ΔG, show that the adsorption process for the two bentonite samples is spontaneous and the degree of spontaneity of the reaction increases with increasing temperature. The increase in adsorption with temperature may be attributed to the increase in the number of active surface sites available for adsorption on the adsorbent and the decrease in the thickness of the boundary layer surrounding the adsorbent with temperature. The values of ΔG are negative for the MCB suggesting that the adsorption process for this material is spontaneous. These results suggest that the internal domains of this sample are suitable environments for Cu(II) cations. Weng et al. [49] noted that ΔG°

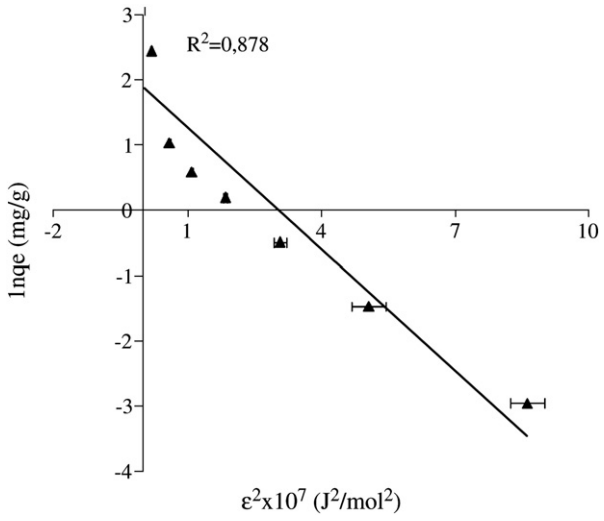

Fig. 4. D–R isotherm plot for adsorption of Cu(II) ions on the MCB sample. $T = 295.15$ K, initial pH = 6.0, $m = 2$ g/L. Error bars represent standard deviations from the average measurements.

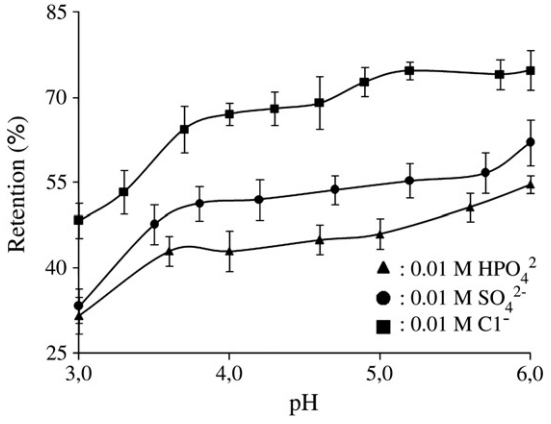

Fig. 6. Adsorption of Cu(II) ions (38 mg/L) by MCB (2 g/L) as function of pH and in the presence of Cl^-, SO_4^{2-}, and HPO_4^{2-}. Error bars represent standard deviations from the average measurements.

Table 5
Thermodynamic parameters for the adsorption of Cu(II) ions onto bentonite samples.

Sample	ΔH (kJ/mol)	ΔS (J/mol K)	ΔG (kJ/mol)			R^2
			303	313	323	
MCB	43.81 ± 5.22	175.85 ± 238	−9.50	−11.25	−10.71	0.969

values up to 20 kJ/mol are consistent with electrostatic interaction between adsorption sites and the metal ion while $\Delta G°$ values more negative than 40 kJ/mol involve charge sharing or transfer from the adsorbent surface to the metal ion to form a coordinate bond. The values of $\Delta G°$ obtained in this work, range from −9.50 to −10.71 kJ/mol indicating that electrostatic interaction may play a significant role in the adsorption process. It may be suggested that a surface complexation reaction is the major mechanism responsible for the Cu(II) ions adsorption process. The negatively charged groups of SiO^-, AlO^- and MgO^- on the MCB surface favor Cu(II) ion adsorptions. The heat of adsorption is positive for MCB sample. The positive value of ΔH indicates the endothermic behavior of the adsorption reaction of Cu(II) ions and suggests that a large amount of heat is consumed to transfer the Cu(II) ions from aqueous into the solid phase. As was suggested by Nunes and Airoldi [50], the transition metal ions must give up a larger share of their hydration water before they could enter the smaller cavities. Such a release of water from the divalent cations would result in positive values of ΔS. This mechanism of the adsorption of Cu(II) ions is also supported by the positive values of ΔS, which show that Cu(II) ions are less hydrated in the bentonite layers than in the aqueous solution. Also, the positive value of ΔS indicates the increased disorder in the system with changes in the hydration of the adsorbing Cu(II) cations.

The average deviations for ΔH and ΔS are roughly 12 and 136%, respectively (Table 5). The source of large errors in determining the thermodynamic parameters may be due to the following reasons: the higher Cu(II) removal due to increasing temperature may be attributed to the interaction taking place between the adsorption sites of MCB and Cu(II). The exchange of the Cu(II) with H^+ needs the bond breaking of OH groups on MCB surfaces, which is an endothermic process. Also, the sorption of Cu(II) requires a diffusion process, which is an endothermic process; i.e., the rise of temperature favors Cu(II) transport within the particles of MCB. Due to these reasons, ΔH, which has little change at low temperatures, displays abrupt decrease and increase at higher temperatures.

Thermodynamic data on Cu(II) ion adsorptions on clays are scarce. Weng et al. [49] have reported that $\Delta H°$, $\Delta S°$ and $\Delta G°$ for the adsorption of Cu(II) ions on spent activated clay have values of 14.51 kJ/mol, 138.78 J/mol K and −26.85 kJ/mol, respectively. Bhattacharyya and Gupta [39] calculated that $\Delta H°$ of Cu(II) ion adsorptions on TBA-montmorillonite, ZrO-kaolinite and montmorillonite is 29.2, 50.5 and 50.7 kJ/mol, respectively, for the temperature range 303–313 K. Lin and Juang [51] have found that ΔH, ΔS and ΔG for Cu(II) ion adsorptions on surfactant modified montmorillonite are 7.05 kJ/mol, 9.09 J/K mol and −9.66 kJ/mol, respectively. Yavuz et al. [52] have reported that $\Delta H°$, $\Delta S°$ and $\Delta G°$ for the adsorption of Cu(II) on kaolinite are 39.52 kJ/mol, 0.117 J/K mol and 4.61 kJ/mol, respectively.

3.6. The mechanism of the adsorption of Cu(II)

Some recent studies have provided evidences about the mechanism of cation adsorption on magnesium oxide [53–59]. In addition to these proofs, other experimental evidences must be considered. They are as follows: (1) the increment of the amount of adsorbed Cu(II), as pH value rises. (2) The fact that the effect of ionic strength on Cu(II) adsorption may be explained by the formation of outer-sphere complexes since K^+ in the background electrolyte competes with the Cu(II) adsorbed on the outer-sphere adsorption sites. In view of the fact pointed out above, it is evident that magnesium oxide modification enhanced the sorption of Cu(II) significantly. It may be explained by considering the coordinative environments of copper ions and surface hydroxyl groups in hydrated surfaces [56–58]. The use of MgO is described acting as a buffering stabilizer agent minimizing heavy metals solubility and avoiding the redissolution [59].

The complex reactions of Cu(II) with MCB may be written as follows (S: MCB surface):

$$S\text{–}OH + Cu^{2+} \rightarrow (S\text{–}O\text{–}Cu)^+ + H^+ \quad (10)$$

$$S\text{–}O^- + Cu^{2+} \rightarrow (S\text{–}O\text{–}Cu)^+ \quad (11)$$

$$2(S\text{–}OH) + Cu^{2+} \rightarrow (S\text{–}O)_2Cu + 2H^+ \quad (12)$$

$$2(S\text{–}O^-) + Cu^{2+} \rightarrow (S\text{–}O)_2\text{–}Cu \quad (13)$$

$$S\text{–}OH + Cu^{2+} + H_2O \rightarrow S\text{–}OCuOH + 2H^+ \quad (14)$$

4. Conclusions

This research demonstrates a preparation method for modifying bentonite with magnesium oxide for use in Cu(II) ion removals. The adsorption of Cu(II) ions by bentonite samples was influenced by pH, ionic strength, and the presence of Cl^-, SO_4^{2-} and HPO_4^{2-}. The adsorption of Cu(II) ions depend upon the nature of the adsorbent surface and the species distribution of Cu(II) ions in solution, which mainly depends on the pH of the system. The adsorption isotherm studies indicate that the adsorption of Cu(II) ions follows both Langmuir and Freundlich isotherms. The values of the adsorption coefficients indicate the favourable nature of adsorption of Cu(II) ions on the MCB. From the values of Langmuir monolayer capacity, q_m, it is concluded that the treatment with magnesium oxide does increase the number of adsorption sites to a large extent. This improvement in bentonite performance may be attributed to an increase in surface charge due to the formation of magnesium oxide on the bentonite surface.

Nomenclature

RB	raw bentonite;
C_e	equilibrium concentration of the adsorbate in the solution (mg/L);
IS	Ionic strength;
K_L	constant that represents the energy or net enthalpy of adsorption (L/mg);
K_F	Freundlich constant indicative of the adsorption capacity of the adsorbent (mg/g);
MCB	magnesium oxide-coated bentonite;
m	mass of adsorbent (g/L);
n	experimental constant indicative of the adsorption intensity of the adsorbent;
q_e	amount of adsorbate removed from aqueous solution at equilibrium (mg/g);
q_m	mass of adsorbed solute completely required to saturate a unit mass of adsorbent (mg/g);

Acknowledgements

The authors thank the Scientific and Technological Research Council of Turkey (TUBITAK) for the financial support (project no. 108T301). They also thank Assoc. Prof. Dr. Yunus Önal in determining porous structures of bentonite samples.

References

[1] S. Veli, B. Alyüz, J. Hazard. Mater. 149 (2007) 226–233.
[2] M. Jiang, X. Jin, Lu. X-Q, Z. Chen, Desalination 252 (2010) 33–39.

[3] M. Doğan, A. Türkyilmaz, M. Alkan, Ö. Demirbaş, Desalination 238 (2009) 257–270.
[4] H. Baker, Desalination 244 (2009) 48–58.
[5] M. Doğan, Y. Turhan, M. Alkan, H. Namli, P. Turan, Ö. Demirbaş, Desalination 230 (2008) 248–268.
[6] M. Sarioglu, U.A. Güler, N. Beyazit, Desalination 239 (2009) 167–174.
[7] N. Ertugay, Y.K. Bayhan, Desalination 255 (2010) 137–142.
[8] A.E. Ofomaja, E.B. Naidoo, S.J. Modise, Desalination 251 (2010) 112–122.
[9] A. Chergui, M.Z. Bakhti, A. Chahboub, S. Haddoum, A. Selatnia, G.A. Junter, Desalination 206 (2007) 179–184.
[10] A. Sarı, M. Tuzen, Desalination 249 (2009) 260–266.
[11] F. Calisir, F.R. Roman, L. Alamo, O. Perales, M.A. Arocha, S. Akman, Desalination 249 (2009) 515–518.
[12] H. Nadaroglu, E. Kalkan, N. Demir, Desalination 251 (2010) 90–95.
[13] I.J. Alinnor, Fuel 86 (2007) 853–857.
[14] P.F. Luckham, S. Rossi, Adv. Colloid Interface Sci. 82 (1999) 43–92.
[15] E. Eren, B. Afsin, Y. Onal, J. Hazard. Mater. 161 (2009) 677–685.
[16] R. Han, W. Zoua, Z. Zhang, J. Shi, J. Yang, J. Hazard. Mater. 137 (2006) 384–395.
[17] R. Han, Z. Lu, W. Zou, W. Daotong, J. Shi, Y. Jiujun, J. Hazard. Mater. B137 (2006) 480–488.
[18] R. Han, W. Zou, H. Li, Y. Li, J. Shi, J. Hazard. Mater. 137 (2006) 934–942.
[19] W. Zou, R. Han, Z. Chen, Z. Jinghua, J. Shi, Colloids Surf. A. Physicochem. Eng. Aspects 279 (2006) 238–246.
[20] B.D. Lee, M.R. Walton, J.L. Megio, Water Res. 39 (2005) 4363–4374.
[21] Y. Xu, L. Axe, J. Colloid Interface Sci. 282 (2005) 11–19.
[22] R. Dohrmann, Appl. Clay Sci. 34 (2006) 31–37.
[23] N.-A.M. Deraz, Thermochim. Acta 421 (2004) 171–177.
[24] R.W. Grimshaw, The Chemistry and Physics of Clays, Ernest Benn Ltd., London, 1971, pp. 968–979.
[25] I. Langmuir, J. Am. Soc. 40 (1918) 1361–1403.
[26] H. Freundlich, J. Phys. Chem. 57 (1906), 385–470.
[27] M.M.B. Dubinin, L.V. Radushkevich, Proc. Acad. Sci. U.S.S.R. Phys. Chem. Sect. 55 (1947) 331–333.
[28] E. Eren, J. Hazard. Mater. 166 (2009) 88–93.
[29] G. Szöllösi, A. Mastalir, M. Bartok, React. Kinet. Catal. Lett. 74 (2001) 241–249.
[30] Ö. Gök, A. Özcan, B. Erdem, A.S. Özcan, Colloids Surf. A. Physicochem. Eng. Aspects 317 (2008) 174–185.
[31] E. Alvarez-Ayuso, A. Garcıa-Sanchez, Environ. Pollut. 125 (2003) 337–344.
[32] H. Chen, Y. Zhao, A. Wang, J. Hazard. Mater. 149 (2007) 346–354.
[33] E. Erdem, N. Karapinar, R. Donat, J. Colloid Interface Sci. 280 (2004) 309–314.
[34] Y.S. Ok, J.E. Yang, Y.-S. Zhang, S.-J. Kim, D.-Y. Chung, J. Hazard. Mater. 147 (2007) 91–96.
[35] S.R. Shukla, R.S. Pai, Sep. Purif. Technol. 43 (2005) 1–8.
[36] M.A.M. Khraisheh, Y.S. Al-Degs, W.A.M. Mcminn, Chem. Eng. J. 99 (2004) 177–184.
[37] H.-J. Fan, P.R. Anderson, Sep. Purif. Technol. 45 (2005) 61–67.
[38] E. Eren, J. Hazard. Mater. 159 (2008) 235–244.
[39] K.G. Bhattacharyya, S.S. Gupta, Sep. Purif. Technol. 50 (2006) 388–397.
[40] Y. El Mouzdahir, A. Elmchaouri, R. Mahboub, A. ElAnssari, A. Gil, S.A. Korili, M.A. Vicente, Appl. Clay Sci. 35 (2007) 47–58.
[41] Y.S. Al-Degs, M.I. El-Barghouthi, A.A. Issa, M.A. Khraisheh, G.M. Walker, Water Res. 40 (2006) 2645–2658.
[42] B.H. Hameed, A.L. Ahmad, K.N.A. Latif, Dyes Pigm. 75 (2007) 143–149.
[43] A. Sarı, M. Tuzen, M. Soylak, J. Hazard. Mater. 144 (2007) 41–46.
[44] D. Xu, X.L. Tan, C.L. Chen, X.K. Wang, Appl. Clay Sci. 41 (2008) 37–46.
[45] A. Sarı, M. Tuzen, D. Cıtak, M. Soylak, J. Hazard. Mater. 148 (2007) 387–394.
[46] A. Gunay, E. Arslankaya, I. Tosun, J. Hazard. Mater. 146 (2007) 362–371.
[47] F. Helfferich, Ion Exchange, McGraw-Hill, New York, 1962.
[48] X. Guo, S. Zhang, X.-Q. Shan, J. Hazard. Mater. 151 (2008) 134–142.
[49] C.-H. Weng, C.-Z. Tsai, S.-H. Chu, Y.C. Sharma, Sep. Purif. Technol. 54 (2007) 187–197.
[50] L.M. Nunes, C. Airoldi, Thermochim. Acta 328 (1999) 297–305.
[51] S.-H. Lin, R.-S. Juang, J. Hazard. Mater. 92 (2002) 315–326.
[52] O. Yavuz, Y. Altunkayank, F. Guzel, Water Res. 37 (2003) 948–952.
[53] H. Yanagisawa, Y. Matsumoto, M. Machida, Appl. Surf. Sci. 256 (2010) 1619–1623.
[54] S. Zhu, H. Hou, Y. Xue, N. Wei, Q. Sun, X. Chen, J. Colloid Interface Sci. 315 (2007) 8–12.
[55] M. Mohapatra, K. Rout, S. Anand, J. Hazard. Mater. 171 (2009) 417–423.
[56] G.R. Bochkarev, G.I. Pushkareva, J. Min. Sci. 34 (1998) 339–343.
[57] G.I. Pushkaryova, J. Min. Sci. 35 (1999) 660–663.
[58] W. Wu, L. Shao, J.F. Chen, S.C. Lu, Fresenius Environ. Bull. 16 (2007) 29–33.
[59] M.A. García, J.M. Chimenos, A.I. Fernández, L. Miralles, M. Segarra, F. Espiell, Chemosphere 56 (2004) 481–491.